



# New Hybrid Material Based on Imidazole-Carboxamide Functionalized Silica for Zn<sup>II</sup> and Pb<sup>II</sup> Removal: Synthesis, Characterization, Isotherms and Kinetics Studies

M. El-Massaoudi<sup>1</sup>, A. Imali<sup>1</sup>, S. Tighadouini<sup>1</sup>, S. Radi<sup>1,2\*</sup>

<sup>1</sup>Laboratory of Applied Chemistry and Environment, Mohammed first University, Oujda, Morocco.

<sup>2</sup>Centre de l'Oriental des Sciences et Technologies de l'Eau (COSTE), Université Med I, Oujda, Morocco.

Received 1 Nov 2017  
Revised 21 Dec 2017  
Accepted 25 Dec 2017

## Keywords

- ✓ Heavy metals,
- ✓ Hybrid material,
- ✓ Silica gel,
- ✓ Langmuir isotherm,
- ✓ Kinetics studies.

## Smaail RADI

[radi\\_smaail@yahoo.fr](mailto:radi_smaail@yahoo.fr) ;  
[s.radi@ump.ac.ma](mailto:s.radi@ump.ac.ma)  
Phone: +212536500601;  
Fax: +212536500603

## Abstract

In this investigation, SiNCI adsorbent was synthesized for heavy metals removal from aqueous solution. The new hybrid material has been prepared by immobilizing a carbonylimidazole system on silica gel previously doped with 3-aminopropyltrimethoxysilane (ATPES). The synthesized sorbent was characterized by AE, SEM, FT-IR and TGA techniques, which confirmed the consummation of the functionalization. Subsequently, the effects of pH of medium and initial concentration of Zn<sup>II</sup> and Pb<sup>II</sup> on adsorption capacity of SiNCI were studied. The experimental data was in accordance with Langmuir adsorption isotherm indicating the formation of a monolayer on the material. The maximum Zn<sup>II</sup> and Pb<sup>II</sup> sorption capacities calculated from Langmuir isotherm are 25.83 mg/g and 10.86 mg/g, respectively. The adsorption process was kinetically explained by the pseudo-second-order kinetic model with high correlation coefficient R<sup>2</sup>= 0.993 and R<sup>2</sup>= 0.992 for Zn<sup>II</sup> and Pb<sup>II</sup>, respectively. It should be noted that SiNCI showed largely enhanced sorption capacity and excellent selectivity towards Zn<sup>II</sup> compared to Pb<sup>II</sup>.

## 1. Introduction

Water is significant for the continuity of human activity. Sadly, toxic heavy metals have damaged water resources through various intermediaries, such as air, food, or heavy metals contained waste. Heavy metals can be distributed into human body and can be accumulated. If this situation continues for a long time, it can be harmful to human health [1-5].

Thus, elimination of toxic metal ions from water resources at trace levels is of the serious importance [6, 7]. Different treatment methods have been used for pre-concentration and separation of metal ions including co-precipitation, ion exchange, liquid-liquid extraction, membrane filtration, and solid-phase extraction (SPE) [8-14]. Solid-phase extraction (SPE) has often been used as a popular technique for extraction and separation of metal ions because of its simplicity, high efficiency, reusability, easy handling, ecofriendly, and the availability of a variety of solid adsorbents [15, 16]. The most significant factor in solid-phase extraction is the selection of adequate adsorbent [6, 17-19]. Many types of adsorbents have been used for the elimination of heavy metal ions from aqueous solutions, such as activated carbon [20], clays [21], chelating resin [22], cellulose [23], chitosan [24], zeolites [25], and silica gel [26-28].

Excellent thermal and mechanical stability, well-modified surface property and relative simple in comparison to polymer resin makes the silica gel an ideal inorganic solid matrix. Also, among the advantages of the silica: its chemical stability, good swelling resistance in different solvents and rapid adsorption kinetics [29, 30]. Many types of functional groups containing oxygen, sulfur and nitrogen groups have been used to make such hybrid materials [31-33].

In this study, silica-gel previously modified with 3-aminopropyltriethoxysilane, was functionalized by 1,1'-Carbonyldiimidazole to obtain SiNCI. The preparation and characterisation by FT-IR, elementary analysis, BET, ATG of the modified silica, and its adsorption properties towards Zn<sup>II</sup> and Pb<sup>II</sup> ions were explored. The effects of pH, shaking time, concentration, kinetics and isotherms adsorption were systematically investigated.

## 2. Material and Methods

### 2.1. Materials and reagents

All solvents and other chemicals (Aldrich, purity >99.5%) were of analytical grades and used without further purification. The silylating agent (ATPES) 3-aminopropyltrimethoxysilane (Aldrich) was used without purification. Silica gel (E. Merck) with particle size in the range of 70-230 mesh, and 60 Å in the median pore diameter, was heated at 120°C during 24 h to activate it before use.

### 2.2. Instrumentation

All metal ions were determined by atomic adsorption measurements and were performed by Spectra Varian A.A. 400 spectrophotometer. The pH value was controlled by a pH 2006, J. P. Selecta; s. a. FT-IR spectra were obtained with Perkin Elmer System 2000. The mass loss determinations were performed in 90:10 oxygen/nitrogen atmospheres on a Perkin Elmer Diamond TG/DTA, at a heating rate of 10°C min<sup>-1</sup>. SEM images were obtained on a FEI-Quanta 200. Elemental analysis was performed by Microanalysis Centre Service (CNRS). The nitrogen adsorption-desorption was obtained by means of a Thermoquest SorpSomatic 1990 analyzer, after the material had been purged in a stream of dry nitrogen. A specific area of modified silica was determined by using the BET equation.

### 2.3. Synthesis of new adsorbents (SiNCI)

First, the silica gel was heated at 120 °C for 24 h to activation. Second, 25g of activated silica gel SiO<sub>2</sub> suspended in 150 mL of anhydrous toluene was refluxed and stirred under nitrogen atmosphere for 2 hours. Then, 10 mL of ATPES (amino-propyl-trimethoxysilane) was added dropwise to this suspension, and the mixture was kept under reflux for 24 hours. The solid was filtered, washed with toluene and ethanol. It was then Soxhlet extracted with a mixture of methanol/ dichloromethane (1/1) for 12h to remove the silylating reagent residue. The immobilized silica gel, named SiNH<sub>2</sub>, was dried in vacuum at room temperature [34]. In the last step, 5 g of SiNH<sub>2</sub> was mixed with 3g of 1,1'-Carbonyldiimidazole in 50 mL methanol for 24h at room temperature. The solid material was filtered, dried and then extracted into Soxhlet with methanol / dichloromethane (1/1) for 12h. The solid material was dried under vacuum at 40 °C for 24 h.

### 2.4. Solid phase extraction technique (Batch method)

The mixture of 10 mg of SiNCI and 10 mL of a metal ion solution at various pH and concentrations was agitated at 25°C until equilibrium was reached. Then, the solid phase was separated by filtration. The remaining metal concentration was determined by atomic absorption spectrometry and the quantity of metal ions sorbed was calculated by the equation (1) [35] :

$$q_e = \frac{(C_0 - C_e) \times m}{V} \quad (1)$$

Where  $q_e$  is the quantity of metal ion on the adsorbent (mg/g),  $C_0$  the initial concentration of metal ions (mg/L),  $C_e$  the equilibrium metal ion concentration in solution (mg/L),  $m$  is the weight of the adsorbent (g),  $V$  is the volume of aqueous solutions (L).

**Effect of concentration:** The suspensions were stirred in the concentration range from 5 to 200 mg/L at 25°C in an thermostat agitator for 120 min. After equilibrium was fixed, the amounts of residual metal ions in solution were measured by atomic absorption spectrometry.

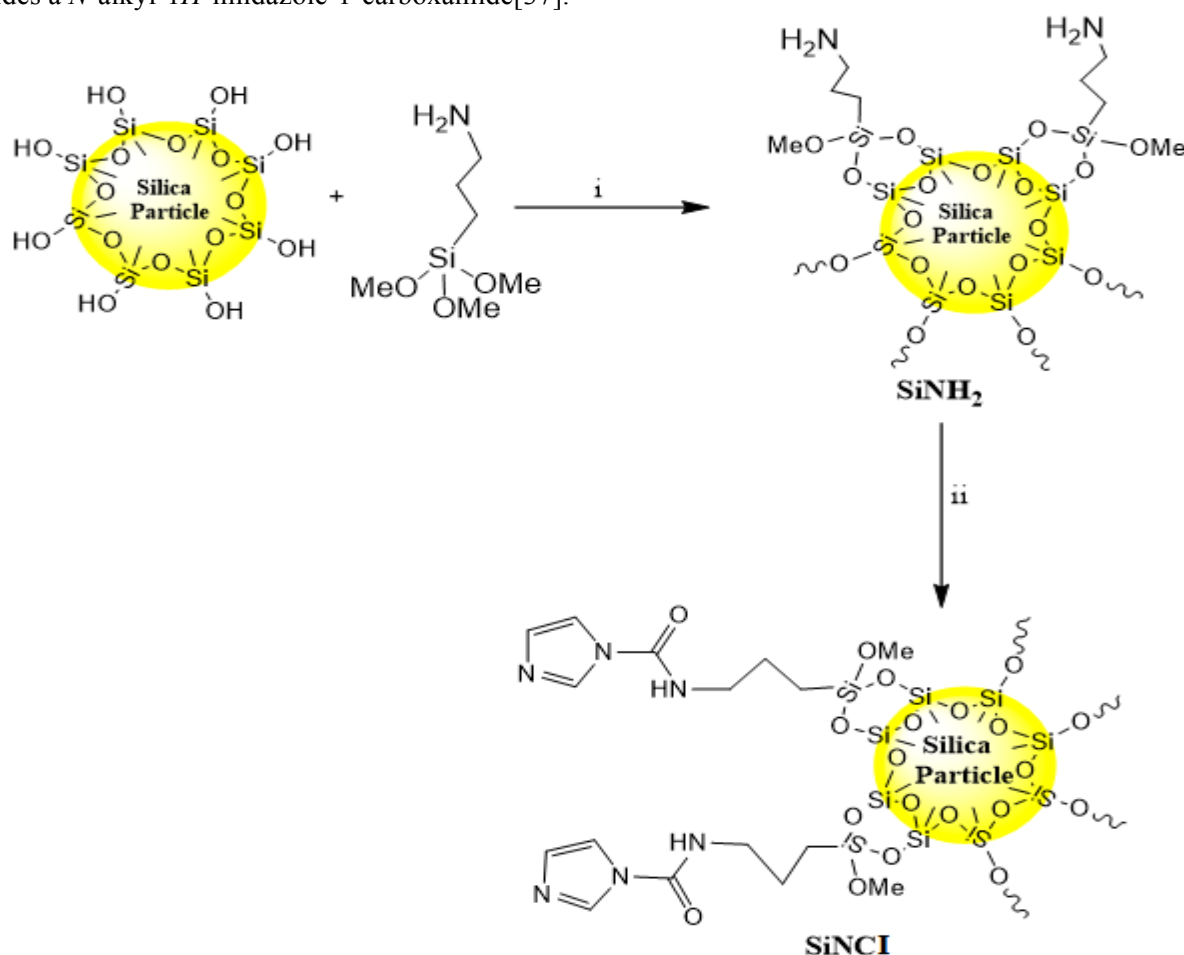
**pH studies:** 10 mg of the material SiNCI was mechanically stirred in solutions of Zn<sup>II</sup> and Pb<sup>II</sup> ions at different pH (2-7) for 30 min. The pH of the solution was adjusted using NaOH and HCl.

**Selectivity experiments:** Ten milligrams of sorbent **SiNCI** was shaken in 10 mL of a solution of  $Zn^{II}$  and  $Pb^{II}$  ions at optimum concentrations of  $55\text{ mg L}^{-1}$  and  $50\text{ mg L}^{-1}$  respectively,  $pH = 6$  and  $25\text{ }^{\circ}\text{C}$ . The mixture was stirred for 30 min.

### 3. Results and discussion

#### 3.1. Preparation of adsorbent **SiNCI**

The first stage in the preparation was the reaction between the silanol groups on the surface of silica and the silylating agent. The **SiNH<sub>2</sub>** material was prepared using our previous reported method [13, 15, 36]. The second stage is the reaction between the solid **SiNH<sub>2</sub>** and 1,1'-carbonyldiimidazole (CDI) in Methanol at room temperature to form the sorbent **SiNCI** as shown in Schema 1. It is known that a reaction of CDI and amine provides a *N*-alkyl-1*H*-imidazole-1-carboxamide [37].



**Schema1:** Synthetic route of the hybrid **SiNAC** (i: Toluene, ii: 1,1'-Carbonyldiimidazole in Methanol).

#### 3.2. Characterization of adsorbent

**Infrared spectroscopy (FT-IR):** The infrared spectra ( $400\text{--}4000\text{ cm}^{-1}$ ) of **SiNH<sub>2</sub>** and **SiNCI** are shown in Figure 1. In the spectrum of **SiNH<sub>2</sub>**, there are three adsorption bands: at  $2941\text{ cm}^{-1}$  representative of the C-H elongation vibrations, at  $1560\text{ cm}^{-1}$  representative of the N-H stretching vibrations assigned to the primary amine, and in the surroundings of  $1400\text{ cm}^{-1}$  representative of Si-C elongation vibrations [15]. In the spectrum of **SiNCI**, the new characteristic bands observed at  $1421$  and  $1549\text{ cm}^{-1}$  can be attributed to the stretching vibration of C=C and C=N groups of the imidazole ring, respectively, while the wide bands around  $2941\text{ cm}^{-1}$  are typical of the stretching vibrations of C-H groups. Moreover, the appearance of the amide groups in the modified hybrid solid was confirmed by the characteristic bands visible at  $1645\text{ cm}^{-1}$  (C=O stretching), and  $1559\text{ cm}^{-1}$  (NH band of amide). These peaks clearly indicate the successful introduction of amide groups into the mesoporous silica.

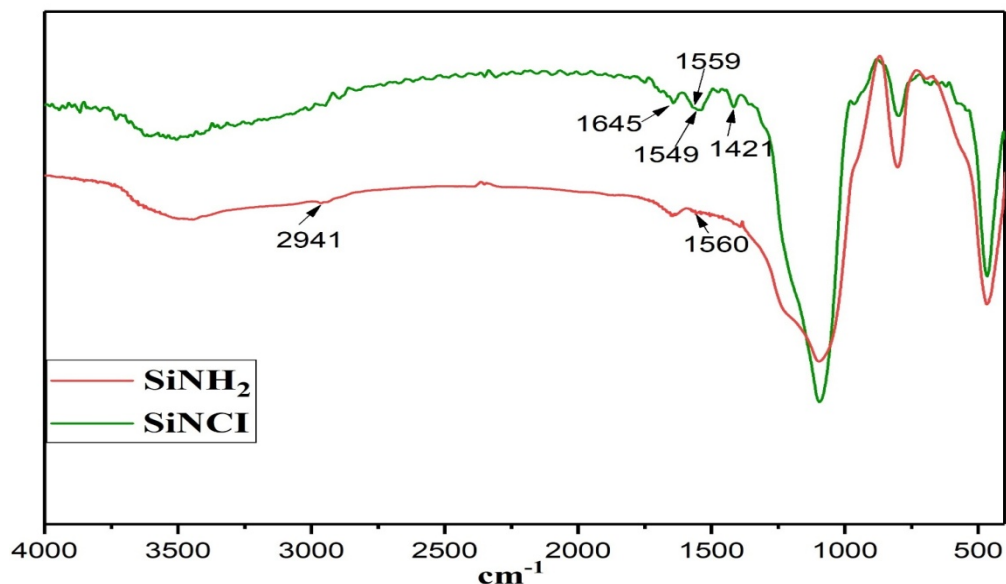


Fig. 1 FT-IR spectra of SiNH<sub>2</sub> and SiNCI.

**Elemental analysis:** The amount of carbon and nitrogen contents (%C = 4.46, %N = 1.66) in SiNH<sub>2</sub> are an indication of a successful functionalization of 3-aminopropyl on the activated surface of silica gel [22]. The increase in amount of carbon and nitrogen in SiNCI (%C = 6.95, %N = 1.92) indicates that the imidazolecarboxamide is attached to SiNH<sub>2</sub>.

**SEM analysis:** The material surfaces were characterized by scanning electron microscopy. The SEM images of SiNH<sub>2</sub> and SiNCI are presented in Figure 2. The surface of SiNH<sub>2</sub> is constituted of a particle structure with deposits on the surface. After the modification by 1,1'-carbonyldiimidazole on SiNH<sub>2</sub>, the surface morphology was changed by the formation of more deposits on its surface attributed to the immobilization of carbonylimidazole units.

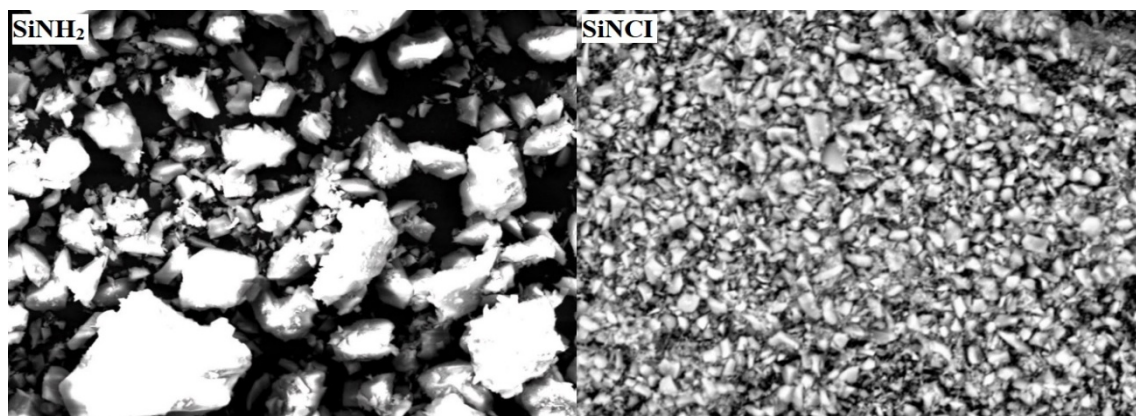


Fig. 2. SEM of the surface of SiNH<sub>2</sub> and SiNCI.

**Thermogravimetric analysis (TGA):** Fig. 3 presents the TGA of SiNH<sub>2</sub> and SiNCI materials. The thermogram of SiNH<sub>2</sub> shows two stages: the first stage with a small mass loss of 1.56% between 25-100 °C assigned to water elimination, and the second stage with a mass loss of 7.47% between 208-800 °C, which corresponds to the 3-propylamine added onto the surface over immobilization. In addition, the curve involving SiNCI shows a marked mass loss of 13.32%, after the exclusion of physisorbed H<sub>2</sub>O. This mass loss is attributed to the decomposition of the grafted organic fraction at the same time the condensation of the remaining silanol groups. The increase of the mass loss is in accordance with the increase of the organic matter attached, in a covalent manner, on the surface of silica gel [38]. The results indicated that the SiNCI sorbent was stable at temperature below 120 °C.

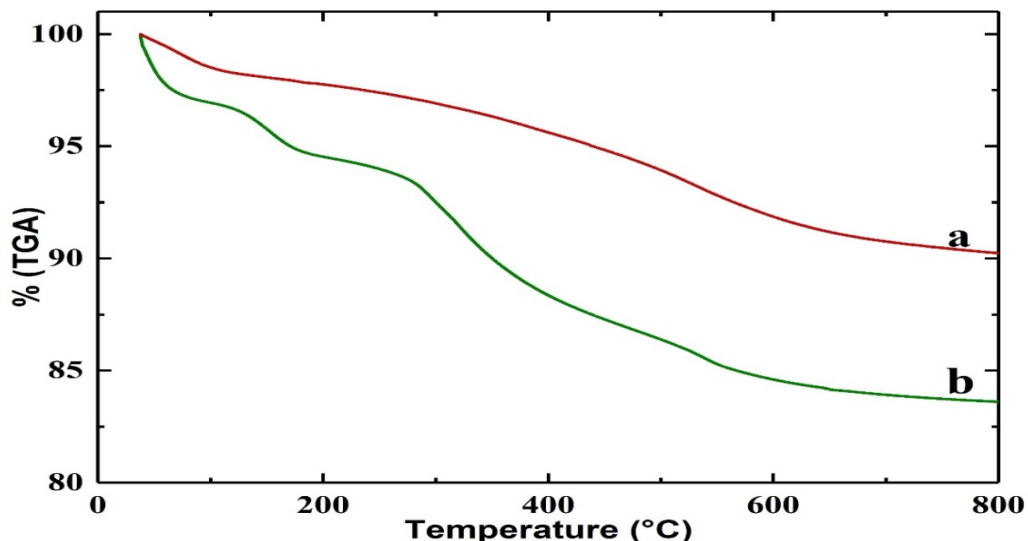


Fig. 3: The thermograms of (a) SiNH<sub>2</sub> and (b) SiNCI

### 3.3. Adsorption studies

#### 3.3.1. Effect of pH

The pH has a significant influence on the adsorption process by the affectation of protonation of donor groups on the surface of the adsorbent. Figure 4 shows that the adsorption continued to increase from pH 2 till optimum pH 6. The adsorption process of Zn<sup>II</sup> and Pb<sup>II</sup> in acidic pH was not optimal. The surface of the adsorbent has positively charged, so the adsorbent surface rejected to bind metal ions. In addition, the electrostatic repulsion between the metal ions and the positively charged donor groups can prevent adsorption of Zn<sup>II</sup> and Pb<sup>II</sup> by the adsorbent[39]; these phenomena caused the low adsorption of Zn<sup>II</sup> and Pb<sup>II</sup>. At pH 6, the active sites on adsorbents were in the form of neutral, so they had a function as an electron-pair donor. At pH > 7, the adsorption of metal ions decreases due to the formation of hydroxyl metals. Based on the results the optimum pH of Zn<sup>II</sup> and Pb<sup>II</sup> adsorption using SiNCI was at pH 6.

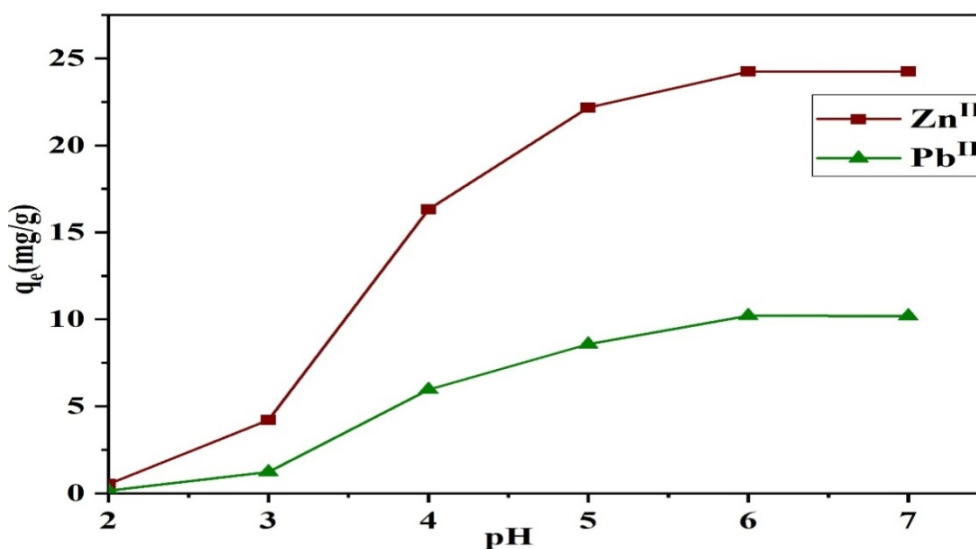


Fig. 4: Effect of pH on the retention of Zn<sup>II</sup> and Pb<sup>II</sup> onto SiNCI.

#### 3.3.1. Effect of contact time and kinetic adsorption

The sorption capacity of Zn<sup>II</sup> and Pb<sup>II</sup> ions was determined as a function of time to determine an optimal contact time for the sorption of metal ions on the sorbent. Figure 5 shows that the Zn<sup>II</sup> and Pb<sup>II</sup> removal increased rapidly over the initial 20 min. After that, the removal rate decreased slightly until the point of equilibrium was achieved at approximately 25 min. The adsorption equilibrium can be achieved rapidly due to the requirement of minimal activation energy.

To better understand the  $Zn^{II}$  and  $Pb^{II}$  adsorption kinetics of SiNCl, theoretical kinetic models such as the pseudo-first-order and pseudo-second-order kinetic models[40-42] have been applied to the experimental data. The pseudo-first-order kinetic model is given by Eq. (2):

$$q_t = q_e(1 - \exp(-k_1 t)) \quad (2)$$

The Pseudo-second-order kinetic model is given by Eq. (3):

$$\frac{t}{q_t} = \frac{1}{k_2 q_e^2} + \frac{t}{q_e} \quad (3)$$

Where  $q_e$  and  $q_t$  are the adsorption capacities for the metal ions (mg/g) in equilibrium and at time  $t$  (min.), respectively,  $k_1(\text{min}^{-1})$  is the kinetic constant of pseudo-first-order model and  $k_2$  (g/mg.min) is the kinetic constant of pseudo-second-order model.

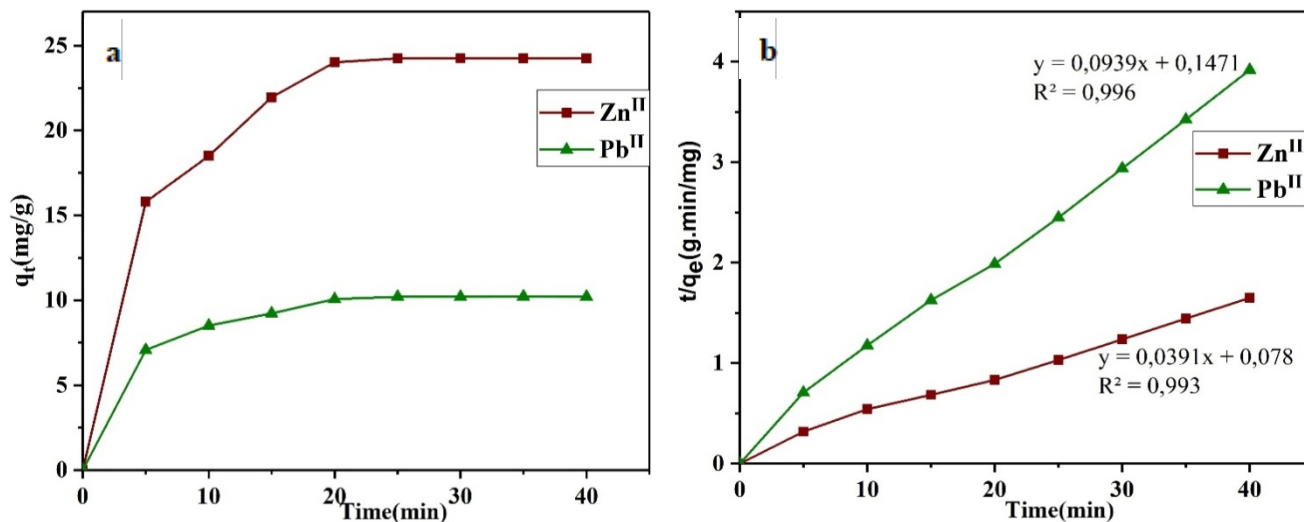


**Fig.5:** a) Effect of shaking time on the adsorption of  $Zn^{II}$  and  $Pb^{II}$  onto SiNCl, b) Pseudo-second-order kinetic model dose: 10 mg,  $V = 10$  mL, and  $pH = 6$  for  $Zn^{II}$  and  $Pb^{II}$  at  $25$  °C.

The parameters of pseudo-first order and pseudo-second order kinetic are indicated in Table 1 and Figure 5. The correlation coefficient of the pseudo-first order was less high than the pseudo-second order kinetic model ( $R^2 = 0.993$ ;  $R^2 = 0.996$ ) for both  $Zn^{II}$  and  $Pb^{II}$  ions respectively, indicating that the adsorption completely was conform with the pseudo-second order reaction and the chemical interaction process controlled the adsorption process. In addition, the experimental  $q_e$  values is close to the theoretical  $q_e$  values found from the second-order kinetic model.

**Table. 1:** Parameters of the pseudo-first order and the pseudo-second order kinetic.

Metal ions	$q_e$ (exp) (mg/g)	First-order			Second-order		
		$q_e$ (mg/g)	$k_1(\text{min}^{-1})$	$R^2$	$q_e$ (mg/g)	$k_2$ (g/mg.min)	$R^2$
$Zn^{II}$	24.25	24.21	0.179	0.988	25.57	0.019	0.993
$Pb^{II}$	10.21	10.11	0.213	0.992	10.64	0.059	0.996

### 3.3.2. Effect of concentration and sorption isotherms

The adsorption capacity is a major factor to determine how much of sorbent is necessary to quantitatively concentrate the analytes from a given solution. As can we see in Figure 6, the uptake amount of adsorption of  $Zn^{II}$  and  $Pb^{II}$  increased with the initial concentrations of  $Zn^{II}$  and  $Pb^{II}$  in solution. The initial  $Zn^{II}$  and  $Pb^{II}$  concentrations were increased until the equilibrium values of 24.25 mg/g and 10.21 mg/g were obtained, respectively. The equilibrium isotherms are very important for understanding the sorption systems; many isothermal equations exist to analyze the experimental equilibrium sorption data. The Langmuir and Freundlich

isothermal equations are the most frequently used for sorption[43, 44]. Herein, the experimental data obtained by the effect of the initial concentration on the sorption capacity were adjusted to the Langmuir and Freundlich sorption isotherms.

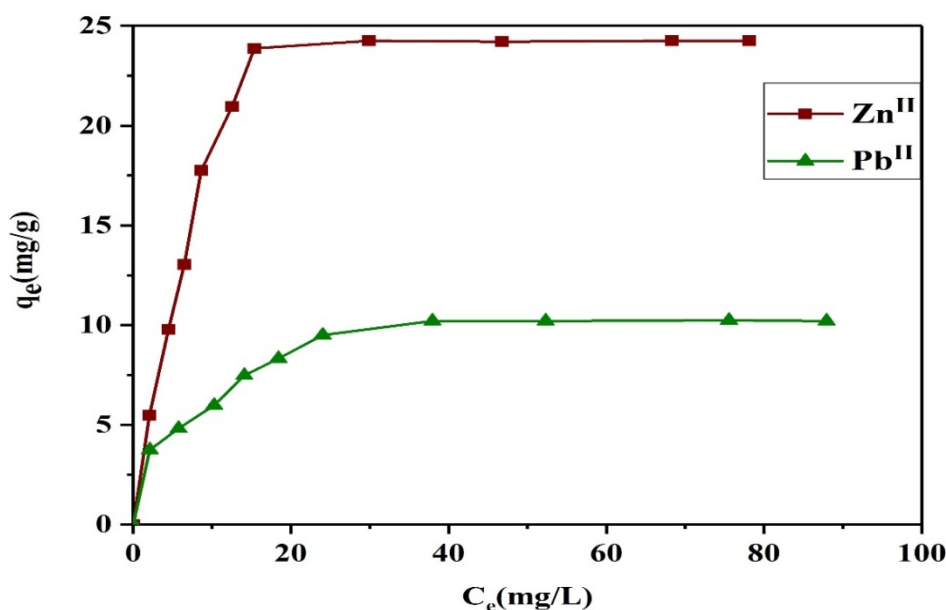


**Fig. 6:** Effect of the concentration on the metal ion adsorption onto SiNCI adsorption dose: 10 mg, V = 10 mL, and pH = 6 for Zn<sup>II</sup> and Pb<sup>II</sup> at 25 °C.

**Langmuir isotherms:** The equilibrium distribution of metal ions between the solid and liquid phases was represented by the Langmuir isotherm. It is applicable for monolayer sorption onto a surface containing a finite number of identical sites. [45, 46]

The Langmuir adsorption model is described in Eq (4):

$$\frac{C_e}{q_e} = \frac{C_e}{q_e} + \frac{1}{qK_L} \quad (4)$$

Where  $q_e$  is the amount of solute sorbed on the surface of the sorbent (mg/g),  $C_e$  is the equilibrium ion concentration in the solution (mg/L),  $q$  is the saturated adsorption capacity (mg/g) and  $K_L$  is the Langmuir adsorption constant (L/mg). The plot of  $C_e/q_e$  vs.  $C_e$  for the sorption gives a straight line of slope  $1/qK_L$  and intercept  $1/q$ .

**Freundlich isotherms:** The Freundlich isotherm is based on the assumption that sorption happens on heterogeneous surfaces with multilayer adsorption [15].

The Freundlich isotherm model can be described as Eq. (5):

$$\ln q_e = \ln k_F + \frac{\ln C_e}{n} \quad (5)$$

Where  $q_e$  is the adsorption capacity (mg/g),  $C_e$  is the equilibrium concentration of the solute (mg/L),  $n$  is the Freundlich constant and  $K_F$  is the binding energy constantly reflecting the affinity of the adsorbent towards metal ions (mg/g).  $K_F$  and  $n$  values, which can be calculated from the intercept and slope of the straight line of  $\ln q_e$  vs.  $\ln C_e$ .

The calculated parameters for the Freundlich and Langmuir models from the linear regressions of the experimental data are summarized in Table 2 and Figure 7. For Zn<sup>II</sup> and Pb<sup>II</sup>, the correlation coefficients got from Langmuir models are  $R^2 = 0.993$  and  $0.992$ , respectively. The SiNCI had a monolayer adsorption capacity value ( $q = 25.83$  mg/g), which was in accordance with the experimentally measured saturation value ( $q_e = 24.25$  mg/g). The Freundlich model had a lower coefficient of determination ( $R^2 = 0.768, 0.913$ ) versus the Langmuir model, which indicated that it was not able to explain the relationship between the quantity of adsorbed Zn<sup>II</sup> and

Pb<sup>II</sup> and its equilibrium concentration in solution. The results indicated that the SiNCI surface was homogeneous and that the adsorption process occurred via monolayers adsorption[47].

**Table 2:** Parameters of isotherm modelsof the adsorption onto SiNCI.

Metal ions	Q <sub>e</sub> exp (mg/g)	Langmuir isotherm model			Freundlich isotherm model		
		q (mg/g)	K <sub>L</sub> (L/mg)	R <sup>2</sup>	n	K <sub>F</sub> (mg/g)	R <sup>2</sup>
Zn <sup>II</sup>	24.25	25.83	0.248	0.992	2.722	6.266	0.768
Pb <sup>II</sup>	10.21	10.86	0.213	0.993	3.403	3.172	0.913

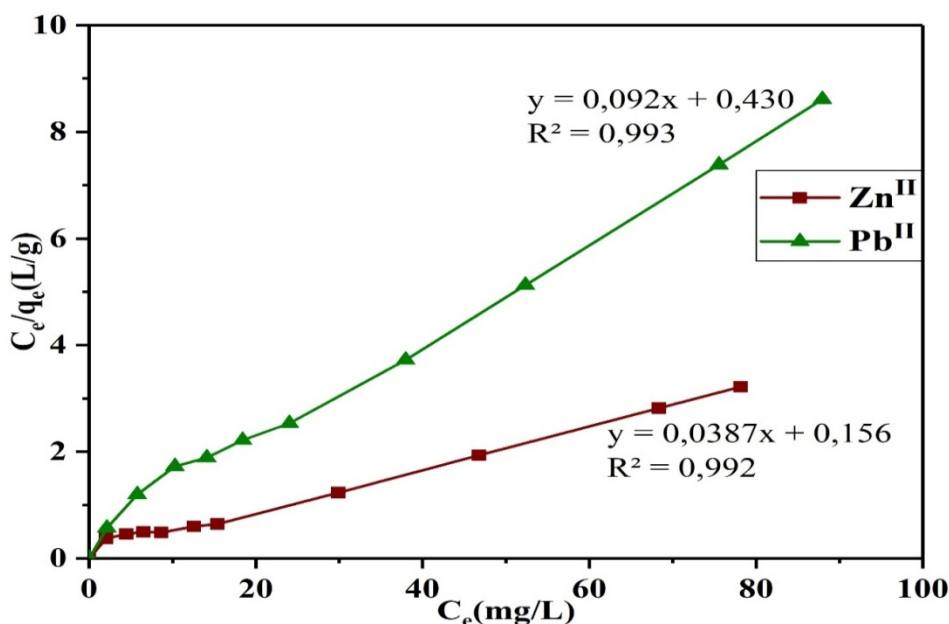


**Fig.7:** Langmuir adsorption model fit of Zn<sup>II</sup>, Pb<sup>II</sup> on SiNAC dose: 10 mg, V = 10 mL, and pH = 6 at 25 °C for Zn<sup>II</sup> and Pb<sup>II</sup>

### 3.3.3. Selectivity studies

Results given in Figure 8 show a quantitative extraction of Zn<sup>II</sup>. Indeed, the adsorption of Pb<sup>II</sup> in the bimetallic solution, is negligible compared to the adsorption of Zn<sup>II</sup>. We noted that the respective concentration of Zn<sup>II</sup> and Pb<sup>II</sup> in the bimetallic system is fixed in the same way as in the mono-metal system. Yet, we notice a selectivity for Zn<sup>II</sup> in the bimetallic solution.

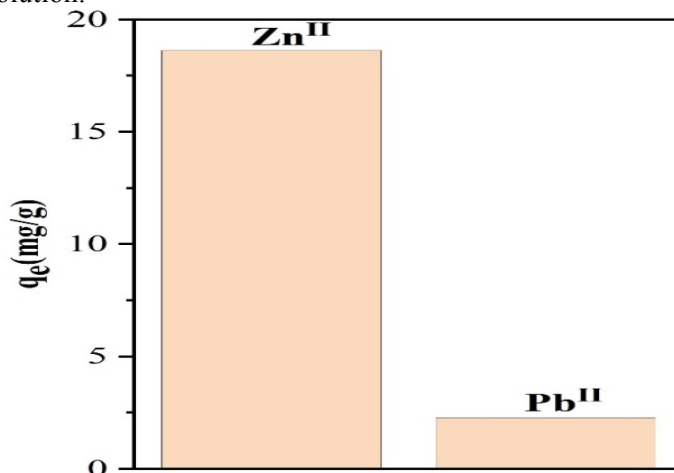


**Fig. 8:** Effect of metal ion selectivity on extraction of Zn<sup>II</sup> and Pb<sup>II</sup> using SiNCI(dose: 10 mg, V = 10 mL and pH = 6 at 25 °C).

### 3.3.4. Comparison with existing adsorbents

Even the comparison of the prepared SiNCI sorbent with the other sorbents in terms of adsorption efficiency was difficult, because of the different experimental conditions; the SiNCI sorbent had been seen to have a relatively high adsorption capacity for Zn<sup>II</sup> over other sorbents already reported in the literature, as shown in Table 3. [16, 33, 35, 48-53].

**Table 3:** Comparison of adsorption efficiency of Zn<sup>II</sup> with previous published adsorbents

Ligand-Silica	Sorption capacity (mg/g)	Refs.
Humicacid	1.51	[16]
1-(Pyrrol-2-yl) imine	24.16	[33]
(Z)-1-(Furan-2-yl) -3-hydroxybut-2-en-1-one	23.36	[35]
C, N-Bipyrazole	0	[48]
2,3-Dihydroxybenzaldehyde	8.69	[49]
p-Toluenesulfonylamide	12.60	[50]
2-Aminomethylpyridine	14.38	[51]
Sulfanilamide	19.09	[52]
3-Aminopropyltriethoxysilane	23.54	[53]
Imidazole-1-carboxamide	24.25	This work

### Conclusions

The next conclusions can be subtracted from the above results: CDI was successfully linked to the surface of silica after modification by 3-aminopropyltrimethoxysilane. The new hybrid material SiNCI was perfectly characterized. All the parameters that can influence the adsorption of Zn<sup>II</sup> and Pb<sup>II</sup> by SiNCI were studied. The optimum pH of the adsorption of the metal ions is 6. The sorption of Zn<sup>II</sup> and Pb<sup>II</sup> ions by the prepared SiNCI can be well expressed with the Langmuir model sorption isotherms which prove the homogeneity of sorbent sorption sites. The kinetics adsorption data were adjusted with various kinetic models; the pseudo-second-order kinetic model was the best model to explain the kinetics of adsorption process. The affinity order of heavy metal ions was as Zn<sup>II</sup>>Pb<sup>II</sup>. The hybrid material described in this work shows further improvement and exhibits better values and greater affinity for the efficient adsorption of Zn<sup>II</sup> over several other sorbents exist in the literature.

**Acknowledgements**—The authors extend their appreciation to the PPR2-MESRSFC-CNRST-P10 project (Morocco).

### References

1. P.B. Tchounwou, C.G. Yedjou, A.K. Patlolla, D.J. Sutton, Heavy metal toxicity and the environment, *Molecular, clinical and environmental toxicology*, Springer 2012, pp. 133-164.
2. M. Jaishankar, T. Tseten, N. Anbalagan, B.B. Mathew, K.N. Beeregowda, *Interdiscip. Toxicol.*, 7(2014)60-72
3. L. Järup, *Br. Med. Bull.*, 68 (2003) 167-182.
4. M. Momodu, C. Anyakora, *Res. J. Environ. Earth. Sci.*, 2 (2010) 39-43.
5. R. Singh, N. Gautam, A. Mishra, R. Gupta, *Indian j. pharmacol.*, 43 (2011) 246.
6. M.E. Mahmoud, M.F. Amira, A.A. Zaghoul, G.A. Ibrahim, *Sep. Purif. Technol.*, 163 (2016) 169-172.
7. H. Sereshti, Y.E. Heravi, S. Samadi, *Talanta*, 97 (2012) 235-241.
8. T.V. Hoogerstraete, B. Onghena, K. Binnemans, *J. Phys. Chem. Lett.*, 4 (2013) 1659-1663.
9. S. Radi, S. Tighadouini, M. Bacquet, S. Degoutin, F. Cazier, M. Zaghrioui, Y.N. Mabkhot, *Molecules*, 19 (2013) 247-262.
10. M. Shamsipur, N. Fattahi, Y. Assadi, M. Sadeghi, K. Sharafi, *Talanta*, 130 (2014) 26-32.
11. H. Bessbousse, N. Zran, J. Fauléau, B. Godin, V. Lemée, T. Wade, M.-C. Clochard, *Radiat. Phys. Chem.*, 118 (2016) 48-54.
12. J.-H. Richard, C. Bischoff, C.G. Ahrens, H. Biester, *Sci. Total. Environ.*, 539 (2016) 36-44.
13. S. Radi, S. Tighadouini, M. Bacquet, S. Degoutin, B. Revel, M. Zaghrioui, *J. Environ. Chem. Eng.*, 3 (2015) 1769-1778.
14. A. Sobianowska-Turek, W. Szczepaniak, P. Maciejewski, M. Gawlik-Kobylińska, *J. Power Sources*, 325 (2016) 220-228.

15. S. Radi, M. El Massaoudi, M. Bacquet, S. Degoutin, N.N. Adarsh, K. Robeyns, Y. Garcia, *Inorg. Chem. Front.*, 4 (2017) 1821-1831.
16. A. Imyim, C. Thanacharuphamorn, A. Saithongdee, F. Unob, V. Ruangpornvisuti, *Desalination Water Treat.*, 57 (2016) 17411-17420.
17. J.-Y. Lee, C.-H. Chen, S. Cheng, H.-Y. Li, *Int. J. Environ. Sci.*, 13 (2016) 65-76.
18. M. Li, M.-y. Li, C.-g. Feng, Q.-x. Zeng, *Appl. Surf. Sci.*, 314 (2014) 1063-1069.
19. D. Mendil, Z. Demirci, O.D. Uluozlu, M. Tuzen, M. Soylak, *Food Chem.*, 221 (2017) 1394-1399.
20. T.A. Saleh, M. Tuzen, A. Sari, *Chem. Eng. Sci.*, 117 (2017) 218-227.
21. L. Karimzadeh, R. Barthen, M. Stockmann, M. Gruendig, K. Franke, J. Lippmann-Pipke, *Chemosphere*, 178 (2017) 277-281.
22. P. Ilaiyaraja, A.S. Deb, D. Ponraju, S.M. Ali, B. Venkatraman, *J. Hazard. Mater.*, 328 (2017) 1-11.
23. F. Wang, Y. Pan, P. Cai, T. Guo, H. Xiao, *Bioresour. Technol.*, (2017).
24. L. Zhang, Y. Zeng, Z. Cheng, *J. Mol. Liq.*, 214 (2016) 175-191.
25. X.-H. Fang, F. Fang, C.-H. Lu, L. Zheng, *Nucl. Eng. Technol.*, 49 (2017) 556-561.
26. S. Radi, S. Tighadouini, M. Bacquet, S. Degoutin, J.-P. Dacquin, D. Eddike, M. Tillard, Y.N. Mabkhot, *Molecules*, 21 (2016) 888.
27. S. Radi, Y. Toubi, M. El-Massaoudi, M. Bacquet, S. Degoutin, Y.N. Mabkhot, *J. Mol. Liq.*, 223 (2016) 112-118.
28. X. Zheng, C. Wang, J. Dai, W. Shi, Y. Yan, *J. Mater. Chem. A*, 3 (2015) 10327-10335.
29. S. Tighadouini, S. Radi, M. El-Massaoudi, M. Bacquet, M. Zaghrioui, *J. Mater. Environ. Sci.*, 5 (2015) 1457-1468.
30. S. Radi, S. Tighadouini, M. Bacquet, S. Degoutin, Y. Garcia, *Anal. Methods*, 8 (2016) 6923-6931.
31. L. Arakaki, V.A. Filha, A. Germano, S. Santos, M. Fonseca, K. Sousa, J. Espinola, T. Arakaki, *Thermochim. Acta.*, 556 (2013) 34-40.
32. B. Kirkan, G.A. Aycik, *J. Radioanal. Nucl. Chem.*, 308 (2016) 81-91.
33. S. Radi, S. Tighadouini, M. El Massaoudi, T. Ben Hadda, M. Zaghrioui, M. Bacquet, J. Daquin, I. Warad, *J. Mater. Environ. Sci.*, 5 (2014) 1280-1287.
34. S. Radi, S. Tighadouini, M. Bacquet, S. Degoutin, L. Janus, Y.N. Mabkhot, *RSC Adv.*, 6 (2016) 82505-14.
35. S. Radi, S. Tighadouini, M. El Massaoudi, M. Bacquet, S.p. Degoutin, B. Revel, Y.N. Mabkhot, *J. Chem. Eng. Data*, 60 (2015) 2915-2925.
36. S. Radi, Y. Toubi, M. Bacquet, S. Degoutin, Y.N. Mabkhot, Y. Garcia, *RSC Adv.*, 6 (2016) 34212-34218.
37. K.J. Padiya, S. Gavade, B. Kardile, M. Tiwari, S. Bajare, M. Mane, V. Gaware, S. Varghese, D. Harel, S. Kurhade, *Org. Lett.*, 14 (2012) 2814-2817.
38. S. Radi, C. El Abiad, N.M. Moura, M.A. Faustino, M.G.P. Neves, *J. Hazard. Mater.*, (2017).
39. L.-Y. Yuan, L. Zhu, C.-L. Xiao, Q.-Y. Wu, N. Zhang, J.-P. Yu, Z.-F. Chai, W.-Q. Shi, *ACS Appl. Mater. Interfaces*, 9 (2017) 3774-3784.
40. Y.-S. Ho, G. McKay, *Process Biochem.*, 34 (1999) 451-465.
41. S. Lagergren, *K.vet.akad.handl*, 24 (1898) 1-39.
42. Y.-S. Ho, *J. Hazard. Mater.*, 136 (2006) 681-689.
43. I. Langmuir, *J. Am. Chem. Soc.*, 3 (1917) 1848-1906.
44. H. Freundlich, *Über die absorption in lösungen*, 1906.
45. S. Uruş, S. Purtaş, G. Ceyhan, F. Tümer, *Chem. Eng. J.*, 220 (2013) 420-430.
46. M.H.P. Wondracek, A.O. Jorgetto, A.C.P. Silva, J. do Rocio Ivassechen, J.F. Schneider, M.J. Saeki, V.A. Pedrosa, W.K. Yoshito, F. Colauto, W.A. Ortiz, *Appl. Surf. Sci.*, 367 (2016) 533-541.
47. M. Dinari, R. Soltani, G. Mohammadnezhad, *J. Chem. Eng. Data*, 62 (2017) 2316-2329.
48. S. Radi, A. Attayibat, M. El-Massaoudi, M. Bacquet, S. Jodeh, I. Warad, S.S. Al-Showiman, Y.N. Mabkhot, *Talanta*, 143 (2015) 1-6.
49. M. Alan, D. Kara, A. Fisher, *Sep. Sci. Technol.*, 42 (2007) 879-895.
50. Q. He, X. Chang, X. Huang, Z. Hu, *Microchim. Acta*, 160 (2008) 147-152.
51. J.A. Sales, F.P. Faria, A.G. Prado, C. Airoidi, *Polyhedron*, 23 (2004) 719-725.
52. X. Zou, Y. Cui, X. Chang, X. Zhu, Z. Hu, D. Yang, *Int. J. Environ. Anal. Chem.*, 89 (2009) 1043-1055.
53. H. Yang, R. Xu, X. Xue, F. Li, G. Li, *J. Hazard. Mater.*, 152 (2008) 690-698.

(2017) ; <http://www.jmaterenvironsci.com>